Implementation of radiative corrections in the first order of α_{em} for the Compton scattering process $\gamma + e^- \to \gamma + e^-$

Primex Note # 42

A. Tkabladze

M. Konchatnyi

Y. Prok

February, 2007

Abstract

This note describes the formalism and method of calculating a radiatively corrected cross section for the Compton scattering process, and the simulation package that can be used to generate final state kinematics for such a process. The BASES/SPRING package was used to create event generators. Two numeric methods of integration were used independently to check the BASES integration results, in good agreement with each other and the NIST database.

Contents

0.1 Formalism

The dynamics of Compton scattering is described by the Klein-Nishina formalism, which takes into account electron spin, and relativistic and quantum effects of QED. The details of derivation can be found in ref [1]. In the lowest order of α_{em}, the scattering process is described by 2 diagrams shown in Fig 1.

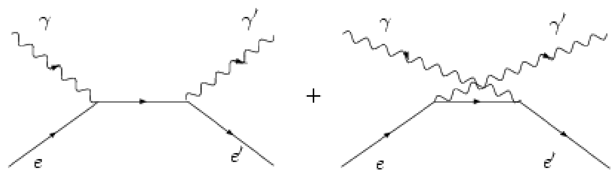

Figure 1: Lowest order Feynman diagrams for $\gamma + e^- \rightarrow \gamma + e^-$ scattering

The differential cross section for Compton scattering depends on the photon incident energy and its scattering angle:

$$\frac{d\sigma}{d\Omega_\gamma} = \frac{r_e^2}{2} \frac{1}{[1+\gamma(1-cos\theta_\gamma)]^2} [1 + cos^2\theta_\gamma + \frac{\gamma^2(1-cos\theta_\gamma)^2}{1+\gamma(1-cos\theta_\gamma)}], \tag{1}$$

where $\gamma = \frac{E_\gamma}{mc^2}$, θ_γ is the photon scattering angle, E_γ is the incident photon energy, m is the electron mass, $r_e =$ is the classical electron radius, and $d\Omega = 2\pi sin\theta d\theta$.

There are two types of corrections (in the first order of α) that need to be applied to the Born cross section. The first type is due to the possibility of emission and reabsorption of a virtual photon by an electron during the scattering process. A typical diagram of such process is shown in Fig. 2, which by interference with diagrams shown in Fig. 1 gives radiative corrections to first order in α. The cor-

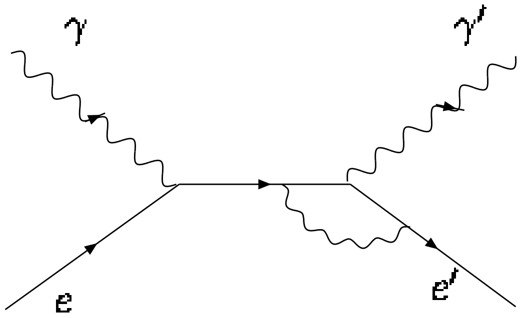

Figure 2: An example of radiative correction

rections were evaluated by Brown and Feynman [4], and are given by equation 35 of ref. [4]. Virtual corrections alone do not have a physical meaning because of the infrared divergence they contain. This is a consequence of the fact that it is impossible to distinguish experimentally between pure elastic and inelastic (accompanied with emission of additional real soft photon) scattering processes.

For this reason another class of corrections which include emission of very soft photons needs to be considered simultaneously with corrections caused by loop diagrams. A typical diagram for such inelastic process is shown in Figure 3.

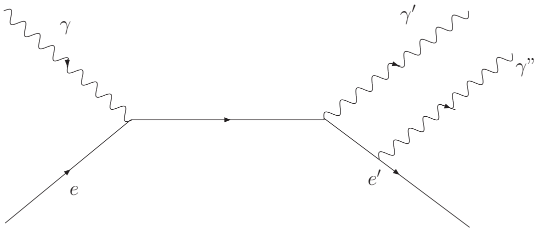

Figure 3: An example of double Compton scattering

The cross section for double Compton scattering where the second photon has energy small compared with the electron mass, $E_\gamma << m_e$, also contains an infrared divergence which cancels the similar divergence in the corrections caused by loop diagram. Corresponding calculations were done to the first order in α, but the multiple Compton scattering of a higher order will also cancel all the radiative infrared divergencies of the same order [4, 5]. For example, the radiative corrections of the order α^2 includes two-loop diagrams, one-loop diagrams with additional real soft photon and diagrams with two real soft photons.

This is physically understandable because experimentally we measure the probability for the Compton process to occur and no other free photons emitted, except for the photons that are not accessible to the experiment. This is equivalent to the probability of a single process plus the probability for the second process in which one of the photons cannot be detected. The class of undetected photons depends on the experimental details, but all experiments have a finite energy resolution so the unaccessible class of photons will have energy less than some value k_{max}. The cross section for the case when one of the emitted photons has energy less than electron mass($k < k_{max} << m_e$) reduces to the Born term (Klein-Nishina) times a factor, and is given by equation 39 of ref. [4]. When corrections due to virtual and real soft photon emission are combined, the divergencies cancel out and we have a physically meaningful finite cross section. The corrected cross section takes the form:

$$d\sigma = d\sigma_0[1 + \delta_{SV}], \tag{2}$$

where the quantity δ_{SV} makes a negative contribution. The measured Compton cross section gets smaller as the experimental resolution improves, which is understandable because more double Compton events are eliminated. δ_{SV}, like the Born term, is still a function of one independent variable, energy or the scattering angle of the hard photon.

Another class of corrections to be considered is the double Compton scattering with secondary photon of energy greater than k_{max}. This process is examined in ref. [5] and [6]. An expression for the differential cross section $\sigma(k; k_1, k_2)dk_1dk_2$ for an incident photon of energy k, striking an electron at rest, to produce one photon with energy in $(k_1, k_1 + dk_1)$, emitted into an element of solid angle $d\Omega_1$ in the direction θ_1, and a second photon with energy in $(k_2, k_2 + dk_2)$ emitted into an element of solid angle $d\Omega_2$ in the direction θ_2, ϕ is derived in ref. [6]. Using conservation of energy and momentum it can be expressed as a function of $k_1, \theta_1, \theta_2, \phi$, where ϕ is the azimuthal angle between the two planes $(\vec{k}, \vec{k_1})$ and $(\vec{k}, \vec{k_2})$:

$$d\sigma(k; k_1, \theta_1, \theta_2, \phi) = \alpha r_0^2 \frac{d\Omega_1 d\Omega_2}{(4\pi)^2} \frac{k_1 k_2 dk_1}{m_2 k} \frac{X}{T_1} \tag{3}$$

X and T_1 are functions of scattering kinematics and are given by equations 9 and 15 of ref. [6]. In this case, the cross section is a function of 4 independent variables,

$k_1, \theta_1, \theta_2, \phi$. The total correction to the Born term will take the form of:

$$d\sigma = d\sigma_0[1 + \delta_{SV} + \delta_{dh}], \tag{4}$$

0.2 Numeric Integration

In order to evaluate the total radiated cross section, we need to carry out integration over the 1-dimensional differential cross section of virtual and soft correction, and the 4-dimensional differential cross section of the hard double compton scattering, and sum the results. The corrections are separated into 2 types based on whether the energy of the secondary emitted photon is less or greater than some energy scale. In other words, it is a parameter, and we call in ω_{2max}, to be consistent with reference [5]. The value of ω_{2max} is small (must be smaller than the mass of electron [8]), but arbitrary otherwise. Since the total cross section is a physically measurable quantity, independent of the choice of parametrization, the final result of integration must be independent of the value of ω_{2max}.

The sum of soft and virtual corrections is given by the equations (4) and (5) of ref. [3], where we replace expression $ln[\frac{2\omega_{2max}}{\lambda}]$ by $ln[\frac{2\omega_{2max}}{m_e}]$ [8]. In order to obtain the total cross section for this process we integrate the equations over the polar angle of the scattered photon, θ and the azimuthal angle, ϕ. In order to obtain the total cross section for double Compton scattering in which both emitted photons might have high energies, we use equation (6.6) of ref. [5], divided by 4 [8, 9], where we integrate over the polar angles of the scattered photons, θ_1, θ_2, azimuthal angle between the 2 emitted photons, $d\phi$, and the energy of one of the emitted photons. The limits of integration over energy are given by the formula (3.4) of ref. [5]. In order to improve the accuracy of 4-dimensional integration, we use variables t_1, t_2 instead of θ_1, θ_2, as it was done in ref. [3]. Parameter ω_{2max} does not enter the formula for differential cross section explicitly but is contained in the limits of integration over energy. All integrations were done using the Monte Carlo method. The integration was carried out with several values of ω_{2max}, for a consistency check. The results for 2 values of ω_{2max} are shown in Table 1.

These results are illustrated in Figure 4. Our conclusion is that the total radiated cross section is independent of the choice of parameter ω_{2max}. We would also like to compare this result with the values obtained from the NIST database. This is done in Figure 5. The blue curve on this plot represents numbers obtained from the XCOMP database of the National Institute of Standards (NIST), under incoherent photon scattering. The incoherent cross sections "were obtained from a combination of the Klein-Nishina formula and nonrelativistic Hartree-Fock incoherent scattering functions. Radiative and double Compton-scattering corrections were also included" (quote from the NIST website). Our calculation is slightly lower than the NIST values,

Table 1: Total Radiated Cross Section

Energy (GeV)	ω_{2max} (GeV)	σ_{SV} (mb)	σ_{DH} (mb)	Total (mb)
3.5	5×10^{-6}	0.2291	0.1479	0.3770
4.0	5×10^{-6}	0.1999	0.1346	0.3346
4.5	5×10^{-6}	0.1772	0.1239	0.3012
5.0	5×10^{-6}	0.1591	0.1150	0.2741
5.5	5×10^{-6}	0.1441	0.1075	0.2517
6.0	5×10^{-6}	0.1318	0.1012	0.2329
3.5	5×10^{-5}	0.2615	0.1155	0.3770
4.0	5×10^{-5}	0.2291	0.1055	0.3346
4.5	5×10^{-5}	0.2039	0.0973	0.3012
5.0	5×10^{-5}	0.1836	0.0906	0.2741
5.5	5×10^{-5}	0.1669	0.0848	0.2517
6.0	5×10^{-5}	0.1530	0.0799	0.2328

by a fraction of a percent. An alternative method of calculation of the total cross section is used in M. Konchatnyi' code [8], where the parameter ω_{2max} is analytically removed from the integration. This method gives results very similar to ours, as illustrated in Figure 6.

Further in this analysis, we use formalism which includes parameter ω_{2max}, which is required by the event generators.

Precision of NIST values is given by the NIST website to be on the order of 5% for this energy range ($\sim$ 5 GeV). A larger error estimate of $\sim$ 20% is quoted by ref. [5], on whose calculation the NIST parametrization is based [8].

Precision of the integration code used to obtain the values in Table 1 is $\sim$ 1%. Precision of integration in BASES is a parameter that can be varied, and it was set to 1 %.

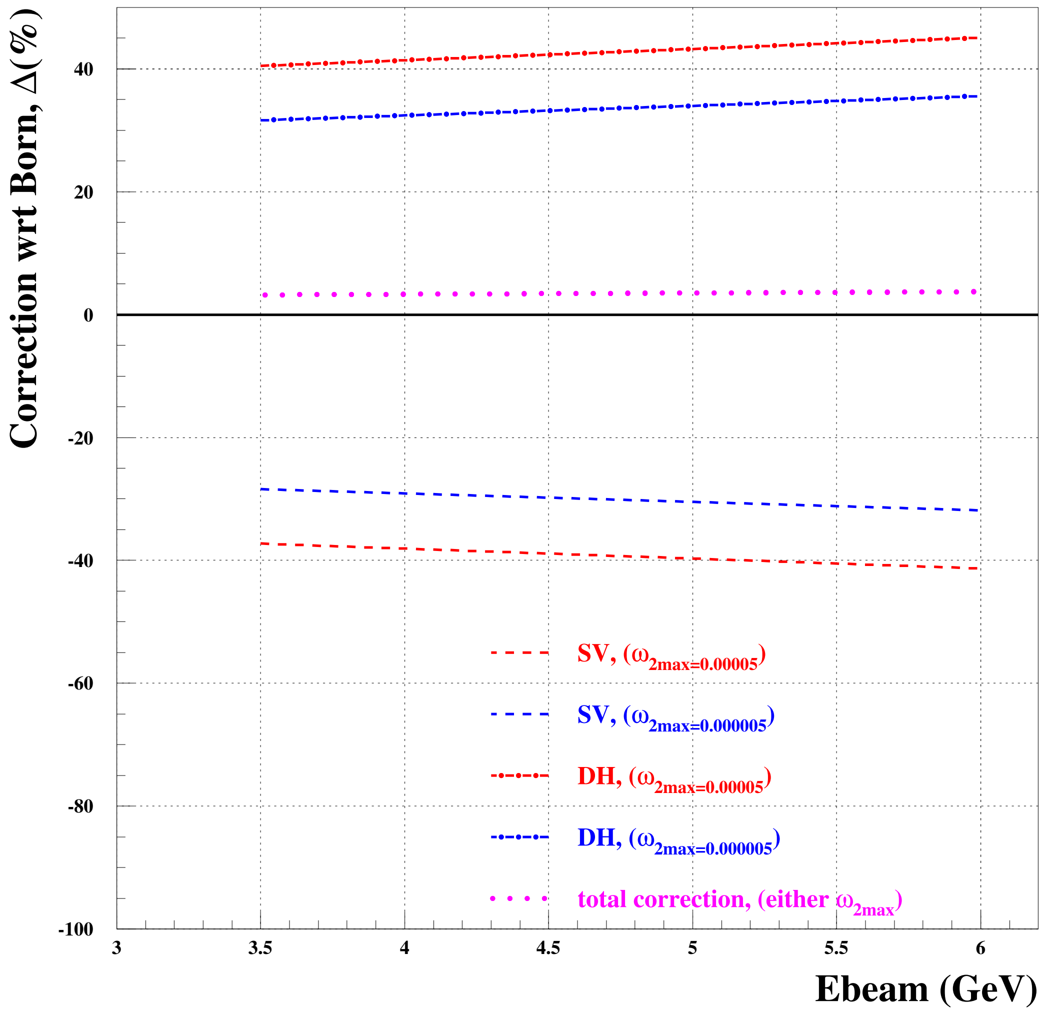

Figure 4: The total radiated cross section is independent of the choice of parameter ω_{2max}

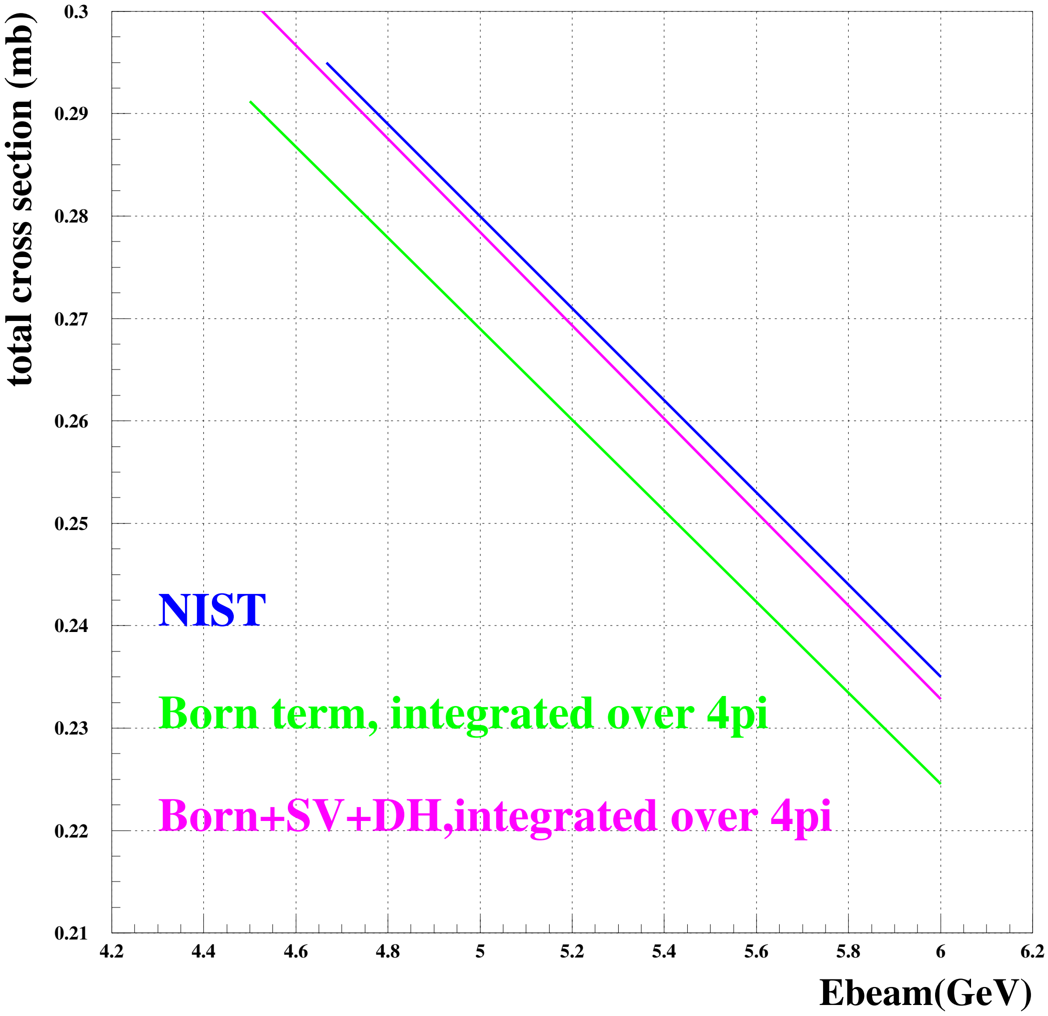

Figure 5: Total radiated cross section obtained by the method outlined above, compared with the Born term (Klein-Nishina) and the NIST parametrization.

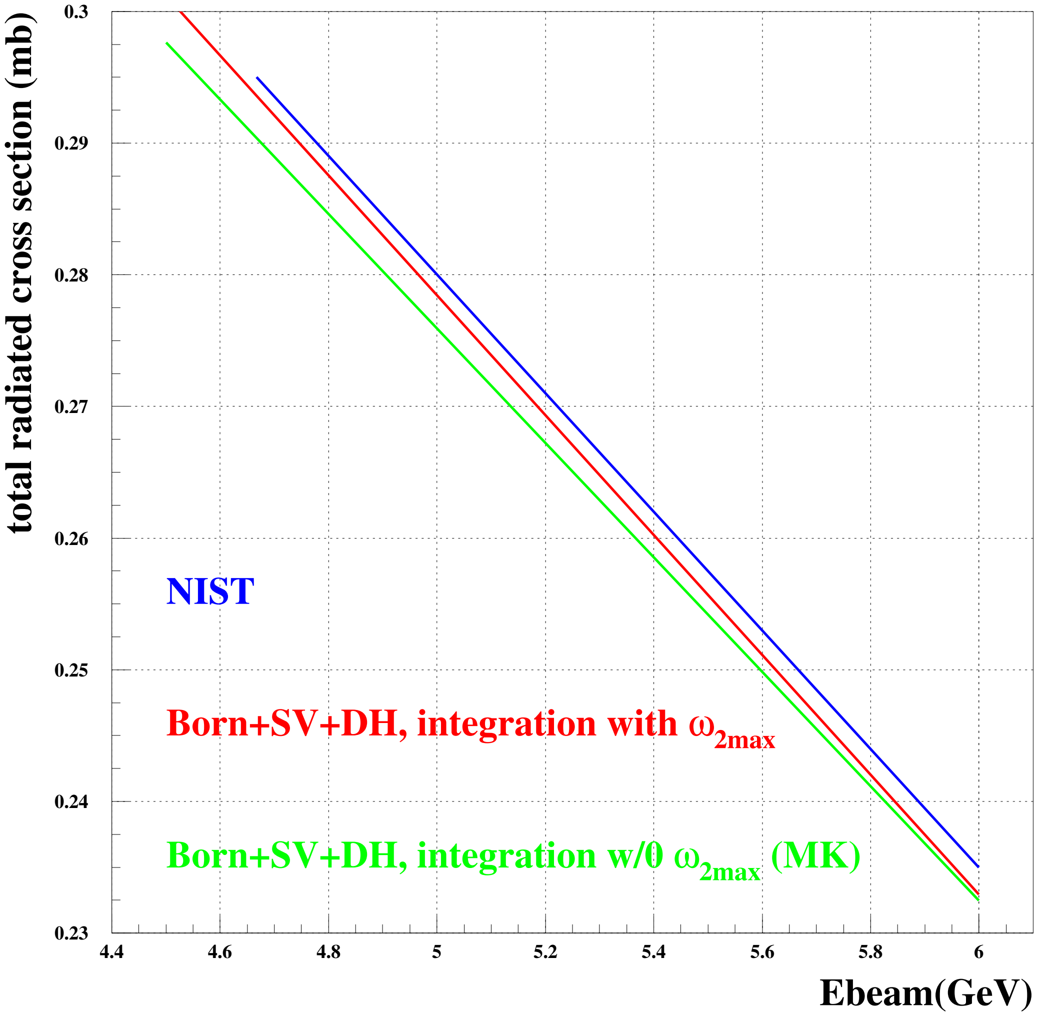

Figure 6: Comparison of the NIST values with 2 methods of integration.

0.3 Simulation Package

Cross section analysis requires the knowledge of efficiency. In order to obtain a realistic 'radiated' efficiency which includes effects of radiative corrections described above, we need to have event generators that generate events according to the full radiated cross section. The event generators were created using the BASES/SPRING simulation package [7, 9]. The BASES/SPRING simulation package is used to obtain total cross sections and to generate events of elementary processes in high energy physics. It is able to integrate singular functions and to generate events with 50 independent variables. This package was used to create 2 generators: one to generate events according to radiatively corrected Klein-Nishina (soft and virtual corrections), and another one to generate events according to the double Compton scattering. Both generators include parameter ω_{2max}. BASES uses the importance and stratified sampling method to integrate the differential cross section, with or without kinematical cuts. The SPRING package uses the probability information supplied by BASES to generate events with four-momentum vectors of final state particles. In our case, we have 2-particle final states for the soft-virtual generator, and 3-particle final states for the double Compton generator. Since we know the relative contribution of each process to the total cross section, we generate events according to that composition.

The simulation package is stored in CVS, under $tools/compton\_rc/bases$.

0.4 Simulated Distributions

In this section we plot some generated quantities to compare data generated with a 'born' generator (shown in black), 'born+soft+virtual' generator (shown in green), and the double compton generator (shown in blue). The initial photon energy was generated in the energy range of 11 production Tcounters, according to $1/E$. This distribution is shown in Figure 7. The elasticity distribution, $\frac{e_{el}+e_{gam}}{ebeam} - 1.$, is shown in Figure 8. While in the case of single Compton scattering, this function is practically a δ-function, the double Compton process produces a 'tail' in the distribution due to the fact that energy in the final state is shared between 3 particles. The energy of generated electrons and photons is shown in Figure 9. The scattering angles of generated electrons and photons is shown in Figure 10.

The 'born' and 'born+SV' processes produce practically the same kinematics, while in the case of the double Compton scattering we observe softer energy distribution of scattered electrons, and more energetic photons in the final state. The occupancies on HyCal are shown in Figure 11 and Figure 12. Figure 11 shows a plot of y vs x for electrons that reached the calorimeter. Figure 12 shows a plot of y_{el} vs y_{gam} for electrons and photons that reached the calorimeter. Figures 11 and 12 were made with a condition that there are at least 2 particles in the final state that do not go through the central hole of the detector.

We can see from these distributions that the geometric acceptance will increase when we include the double Compton process in the calorimeter. This is due to the fact that the electrons are less energetic in case of the double Compton process, and not as many of them will go through the central hole. For calculation of full efficiency, generated data will be propagated through the experimental setup using GEANT-3.

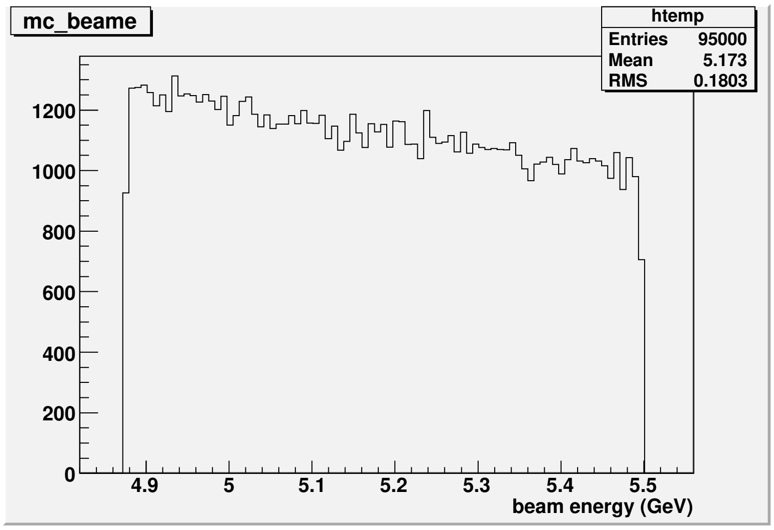

Figure 7: Energy of the initial photon

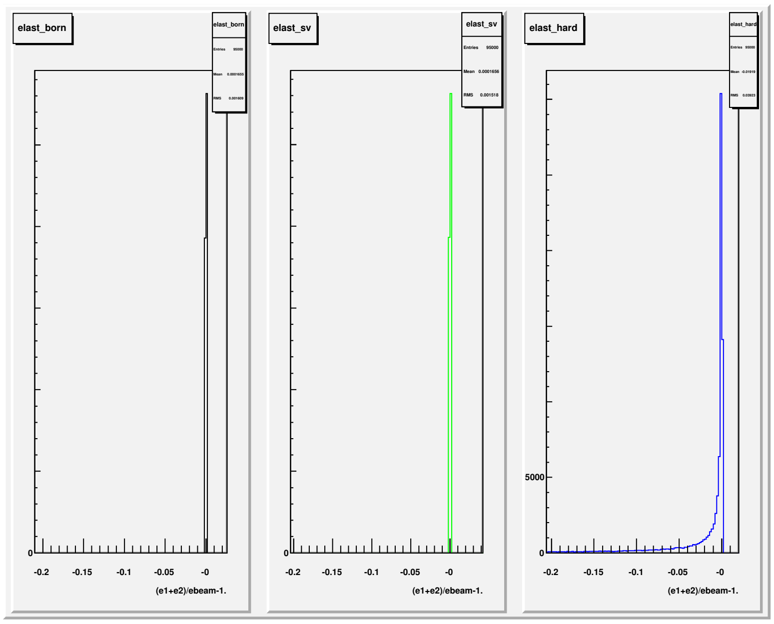

Figure 8: $\frac{e_{el}+e_{gam}}{ebeam} - 1.$. From left to right: born, born+SV, double compton process

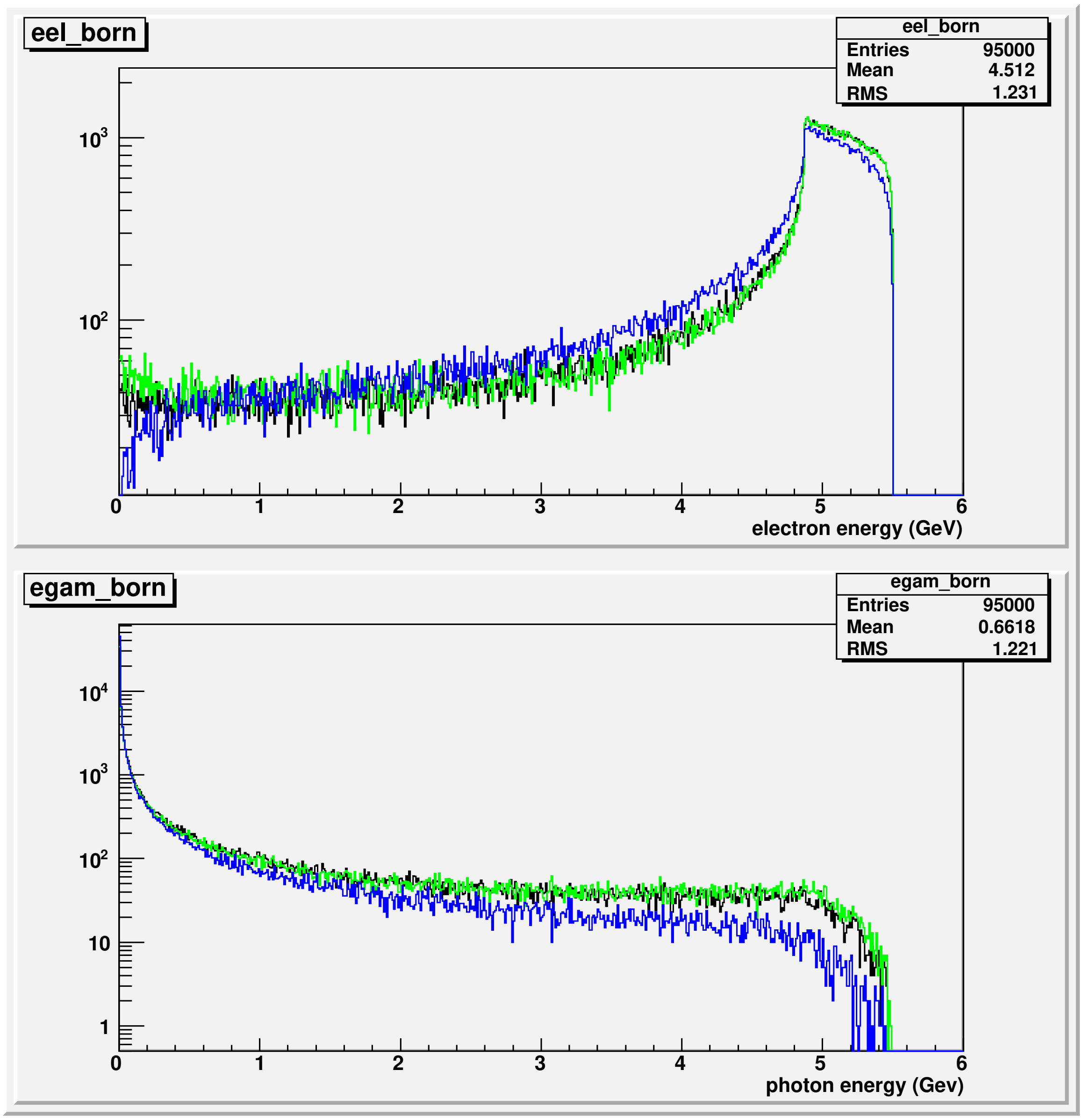

Figure 9: Energy of scattered particles. Top: electrons, Bottom: photons. Color code: black (born), green (born+SV), blue (double compton)

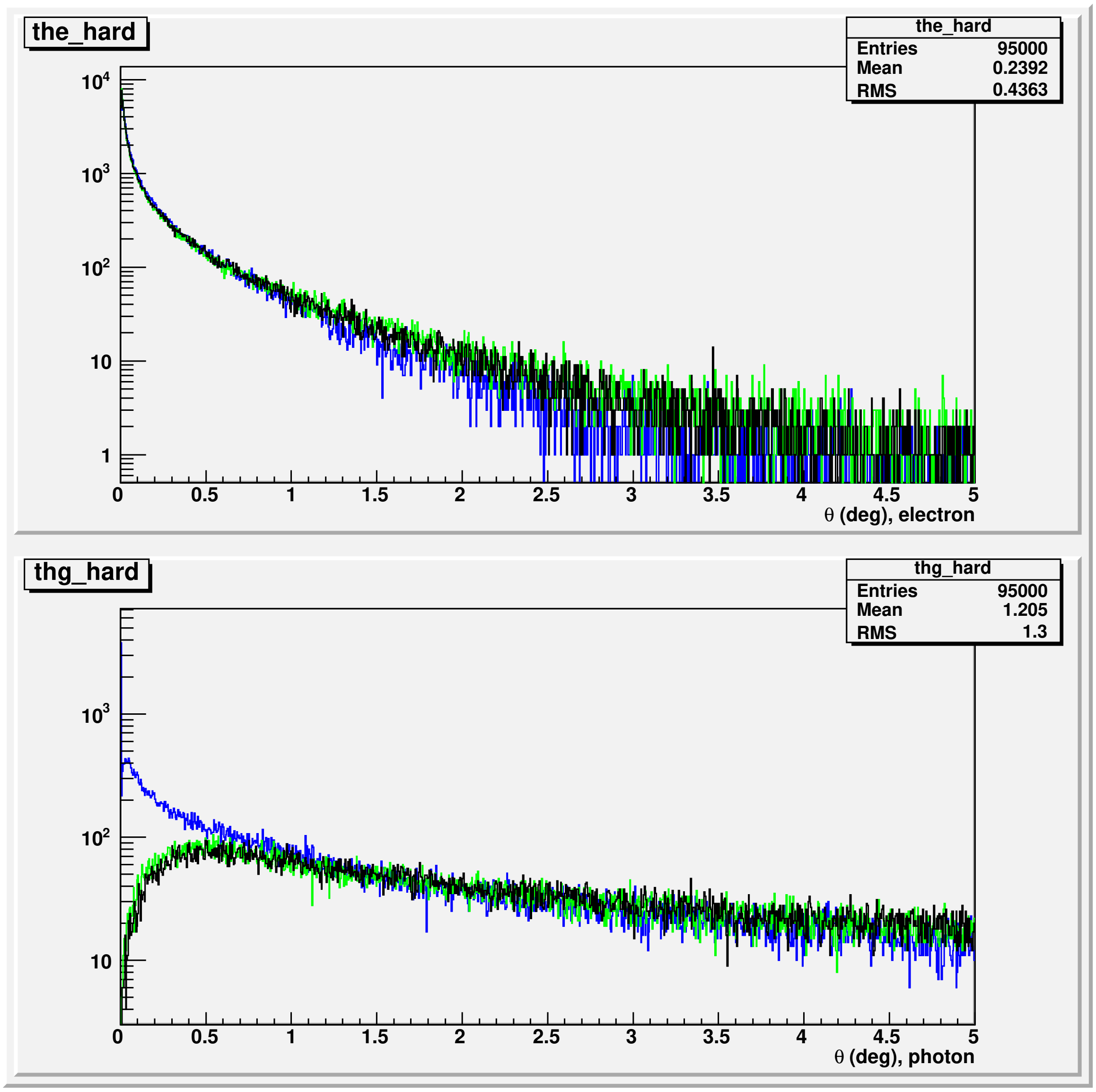

Figure 10: Scattering angle, θ, of generated particles. Top: electrons, Bottom: photons. Color code: black (born), green (born+SV), blue (double compton)

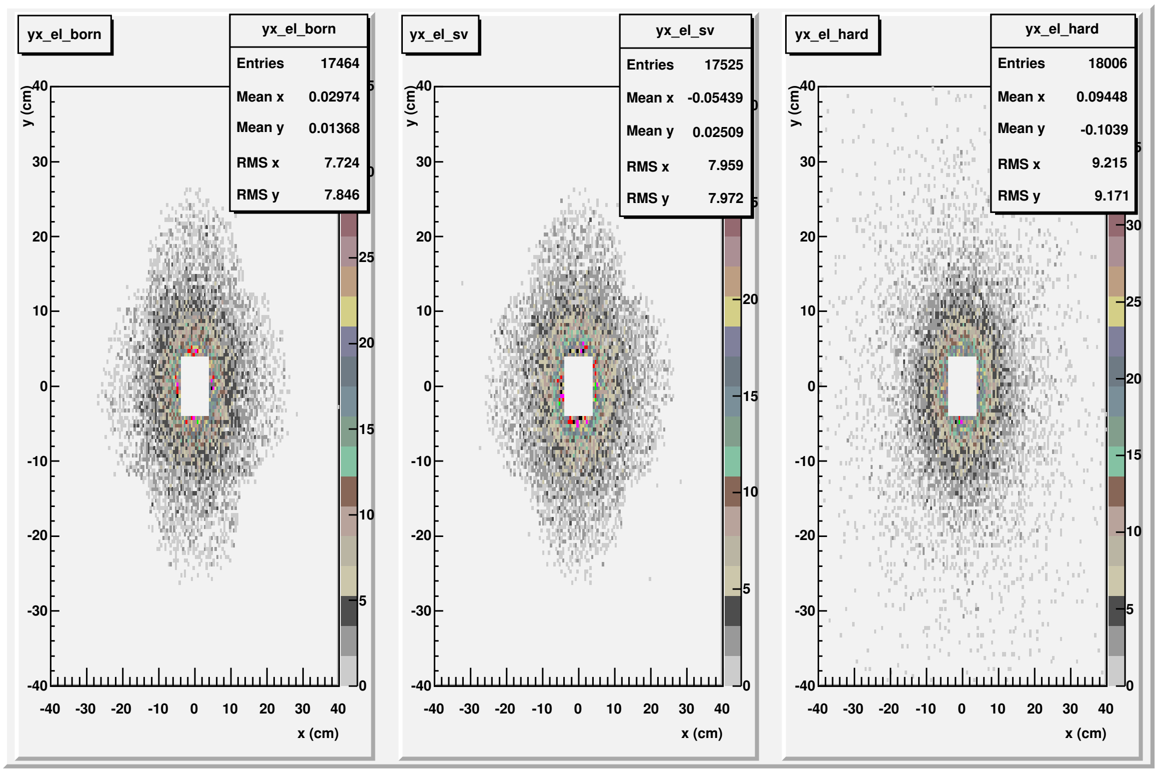

Figure 11: Occupancy of electrons on the calorimeter with the central hole cut out. Left to right: born, born+SV, double compton

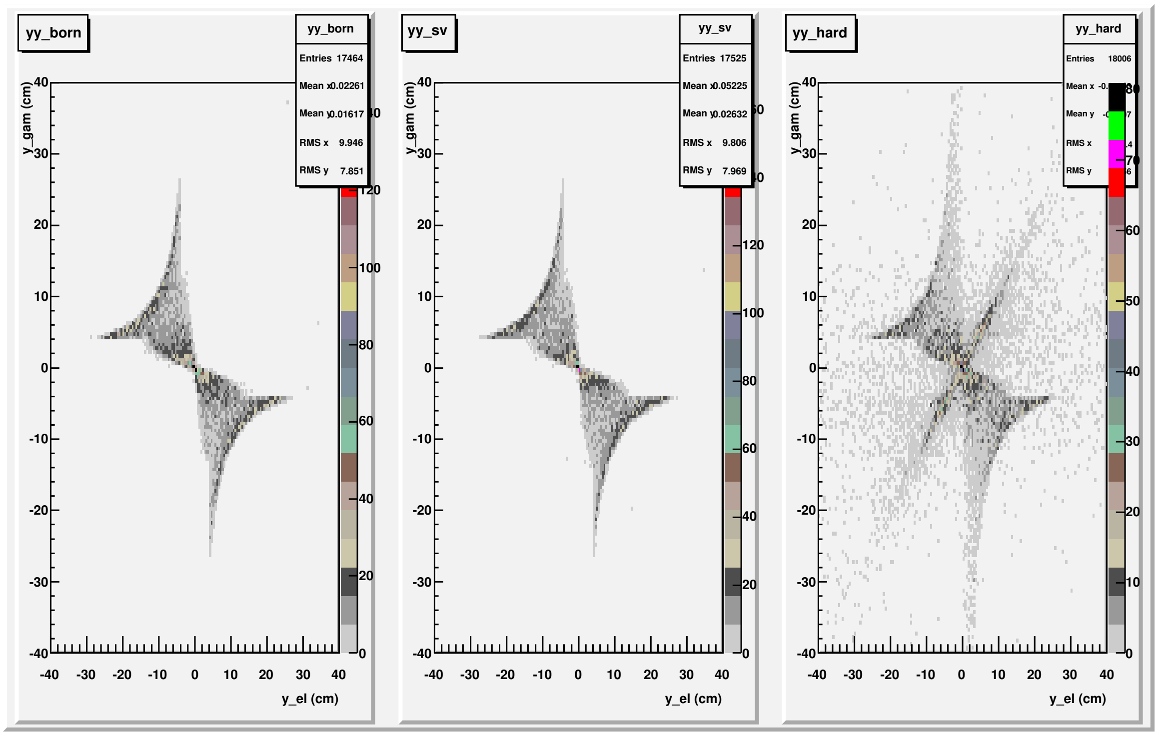

Figure 12: y_{el} vs y_{gam}.Left to right: born, born+SV, double compton

References

[1] M. Peskin and D. Schroeder, *An Introduction to Quantum Field Theory*, (Addison-Wesley Publishing Company) (1995).

[2] A. I. Akhiezer and V. B. Berestetsky, Quantum Electrodynamics, (Nauka, Moscow) (1969).

[3] M. Konchatnyi, *Compton effect in kinematic conditions of PrimEx*, (Primex Note 37) (2006)

[4] L.M.Brown and R.P.Feynman, Phys. Rev. 85, 231 (1952)

[5] K. Mork, Phys.Rev. A4, 917-927 (1971)

[6] F.Mandl and T.H.R. Skyrme, Proc. Roy. Soc. (London) A 215, 497 (1952)

[7] S. Kawabata, Computer Physics Communications 88, 309-326 (1995)

[8] M. Konchatnyi, Private Communication

[9] A. Tkabladze, Private Communication